JOC The Journal of Organic Chemistry

Article

pubs.acs.org/joc

Quantitative First-Principles Kinetic Modeling of the Aza-Michael Addition to Acrylates in Polar Aprotic Solvents

Gilles B. Desmet,[†] Dagmar R. D'hooge,[†,‡] Pinar Sinem Omurtag,[§] Pieter Espeel,[§] Guy B. Marin,[†] Filip E. Du Prez,[§] and Marie-Françoise Reyniers*[,†]

[†]Laboratory for Chemical Technology, Ghent University, Technologiepark 914, B-9052 Gent, Belgium

[‡]Department of Textiles, Ghent University, Technologiepark 907, B-9052 Gent, Belgium

[§]Polymer Chemistry Research Group, Ghent University, Krijgslaan 281 S4-bis, B-9000 Gent, Belgium

Supporting Information

ABSTRACT: This work presents a detailed computational study and kinetic analysis of the aza-Michael addition of primary and secondary amines to acrylates in an aprotic solvent. Accurate rate coefficients for all elementary steps in the various competing mechanisms are calculated using an ONIOM-based approach in which the full system is calculated with M06-2X/6-311+G(d,p) and the core system with CBS-QB3 corrected for solvation using COSMO-RS. Diffusional contributions are taken into account using the coupled encounter pair model with diffusion coefficients calculated based on molecular dynamics simulations. The calculated thermodynamic and kinetic parameters for all forward and reverse elementary reactions are fed to a microkinetic model giving excellent agreement with experimental data obtained using GC analysis. Rate analysis reveals that for primary and secondary amines, the aza-Michael addition to ethyl acrylate occurs preferentially according to a 1,2-addition mechanism, consisting of the pseudoequilibrated formation of a zwitterion followed by a rate controlling amine assisted proton transfer toward the singly substituted product. The alternative 1,4-addition becomes competitive if substituents are present on the amine or double bond of the acrylate. Primary amines react faster than secondary amines due to increased solvation of the zwitterionic intermediate and less sterically hindered proton transfer.

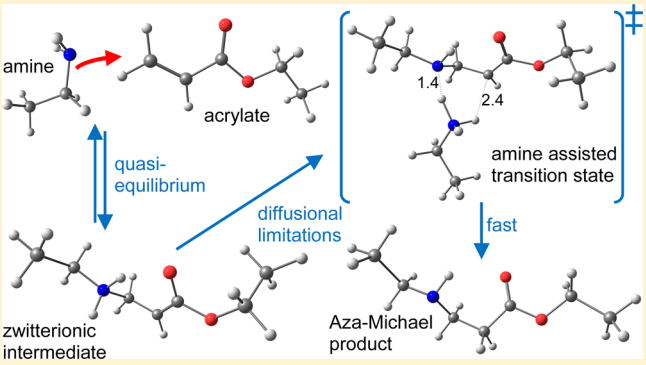

1. INTRODUCTION

The Michael addition, also referred to as 1,4-conjugate addition, is a popular and versatile synthetic method for linking electron poor olefins with a range of nucleophiles. This reaction was described for the first time by Arthur Michael in 1887,[1,2] as the base catalyzed addition of a resonance stabilized carbanion, such as an enolate, the Michael donor, to an activated α,β-unsaturated carbonyl containing compound, the Michael acceptor. Since then, however, the scope has increased drastically and now includes the addition of a broad range of nucleophiles to a conjugated unsaturated compound.[3] The Michael addition thus offers a whole realm of bond formation possibilities next to its originally described use in the formation of carbon−carbon bonds, and is now also widely applied in the formation of oxygen−carbon bonds,[4,5] sulfur−carbon bonds,[6,7] phosphorus−carbon bonds,[8,9] and nitrogen−carbon bonds. This latter reaction is also termed aza-Michael addition, and has been applied plentifully in the synthesis of β-amino acids and derivatives,[10,11] and more recently also in polymer science,[3] e.g., for the synthesis of green building blocks,[12] poly(amino esters),[13,14] polymer networks,[15,16] and block copolymers.[17] A more complete overview of the use of the aza-Michael addition can be found in a comprehensive review by Rulev.[18] Furthermore, the popular thiol-Michael addition[19] is also commonly catalyzed by amines, and therefore side reactions between the amine catalyst and the ene-substrate are possible and could be of concern, e.g., in amine-thiol−ene reaction sequences.[20−22]

The driving force for all types of Michael additions is the same, i.e., the transformation of the π-bond between the doubly bond carbon atoms into a σ-bond between the nucleophile and a carbon atom. In terms of the reaction mechanism, however, a range of options is possible. Weak nucleophiles, such as thiols, will not react unless activated. This happens by deprotonation using a catalyst. Also in the case of stronger nucleophiles, such as amines, heterogeneous catalysis,[23−26] homogeneous organometallic catalysis,[27,28] or organocatalysis[29−33] is widely applied, due to the significantly enhanced rate of reaction.[30] Despite these obvious advantages, the uncatalyzed aza-Michael addition has also found ample use in the synthesis of various mono- and dihydroamination products due to the inherent simplicity of this

Received: September 9, 2016
Published: November 16, 2016

DOI: 10.1021/acs.joc.6b02218
J. Org. Chem. 2016, 81, 12291−12302

Scheme 1. Reaction Network for the Aza-Michael Addition of Diethylamine to Ethyl Acrylate in an Aprotic Solvent[a]

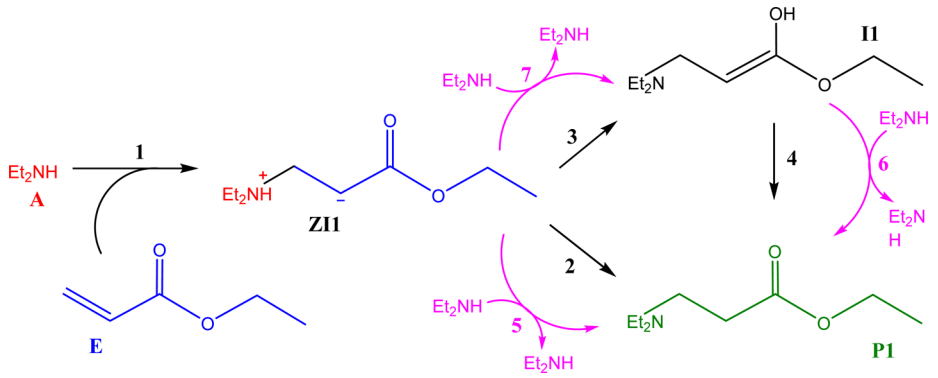

[a]Reactions **1** − **4** are unassisted. Reactions **5** − **7** are assisted reactions in which the amine reactant is involved.

Table 1. Standard Reaction Enthalpy, Entropy, and Gibbs Free Energy[a]; Standard Activation Enthalpy, Entropy, and Gibbs Free Energy[b]; and Forward and Reverse Rate Coefficients (in L mol^{-1} s^{-1} or s^{-1}) at 298.15 K in THF for All elementary Reactions in the Detailed Reaction Scheme of the Aza-Michael Addition of Diethylamine to Ethyl Acrylate[c]

reaction	$\Delta_r H°$	$\Delta_r S°$	$\Delta_r G°$	$\Delta^{‡} H°$	$\Delta^{‡} S°$	$\Delta^{‡} G°$	k_+	k_-
R1	29.5	−123.7	66.4	47.4	−185.3	84.3	2.1×10^{-02}	9.3×10^{09}
R2	−95.1	12.2	−97.5	89.4	−12.0	91.8	1.0×10^{-03}	8.7×10^{-21}
R3	−4.9	−11.1	−2.7	−3.3	−22.6	1.2	7.5×10^{12}	2.5×10^{12}
R4	−90.1	23.3	−94.8	216.7	15.7	213.6	4.7×10^{-25}	1.2×10^{-41}
R5	−95.1	12.2	−97.5	2.6	−182.1	38.8	2.0×10^{06}	1.7×10^{-11}
R6	−90.1	23.3	−94.8	25.1	−162.3	57.4	1.1×10^{03}	2.7×10^{-14}
R7	−4.9	−11.1	−2.7	−5.7	−191.5	32.3	2.7×10^{07}	9.0×10^{06}

[a]$\Delta_r H°$, $\Delta_r S°$, $\Delta_r G°$, in respectively kJ mol^{-1}, J mol^{-1} K^{-1}, kJ mol^{-1}. [b]$\Delta^{‡} H°$, $\Delta^{‡} S°$, $\Delta^{‡} G°$, in respectively kJ mol^{-1}, J mol^{-1} K^{-1}, kJ mol^{-1}. [c]As shown in Scheme 1 (R_1, R_2 = C_2H_5).

approach.[34−39] A first kinetic investigation on an uncatalyzed aza-Michael addition has been performed by Popov et al.[40] The authors studied the addition of primary and secondary aliphatic amines to trans-(2-furyl)nitroethylene in acetonitrile. The formation of a zwitterionic intermediate is hypothesized followed by a proton transfer that might occur over two parallel routes; directly or assisted by a second amine molecule. In a computational investigation by Pardo et al.,[41] the mechanism of the 1,2-addition and the 1,4-addition of ammonia to acrolein and acrylic acid has been described in an aqueous environment, where a water molecule acts as a catalyst in the rate-determining proton transfer step.

However, a detailed kinetic analysis in an aprotic solvent, which is especially relevant in the scope of polymeric applications, has, to the best of our knowledge, not been performed. In this work, various possible competing reaction mechanisms are considered for the aza-Michael addition of both a primary and a secondary amine (ethyl- and diethylamine, respectively) to ethyl acrylate in tetrahydrofuran (THF), an often used aprotic polar solvent in polymer science. The calculated rate coefficients are fed to a microkinetic model to obtain concentration profiles for reactants and products which are compared with experimental data. Rate analysis is used to determine the dominant reaction steps. Furthermore, the influence of methyl-substituents on the double bond is illustrated by comparison with ethyl crotonate and ethyl methacrylate.

2. RESULTS AND DISCUSSION

Aza-Michael Addition with a Secondary Amine. A detailed reaction scheme for the aza-Michael addition of diethylamine to ethyl acrylate in an aprotic solvent is presented in Scheme 1, based on earlier reaction mechanisms postulated by Popov et al.[40] and Pardo et al.,[41] and expanded with additional elementary reactions corresponding to direct keto−enol tautomerization. Also the possible competing aminolysis of the ester group[42] in the acrylate has been examined. However, since the energies involved in this reaction are significantly higher, as shown in Section S3 in the Supporting Information, this reaction is further ignored.

The first step (**1**) is the formation of the zwitterionic intermediate, **ZI1**. This zwitterionic intermediate can then undergo a proton transfer, either to the carbon in α position of the carbonyl group (**2**), resulting in the product **P1** − corresponding to the nucleophilic 1,2-addition, or to the carbonyl oxygen (**3**), resulting in a neutral enol intermediate **I1**, which is the nucleophilic 1,4-addition. The enol intermediate then rearranges to the keto-product via direct keto−enol tautomerization (**4**).

These latter three proton transfer reactions can also occur over an amine-assisted transition state, in which a second secondary amine plays the role of a proton shuttle (reactions **5**, **7**, and **6**, respectively). Because the formed product **P1** is a tertiary amine and hence lacks an N−H bond, it cannot serve as an assisting molecule in the proton transfer reactions.

Using diethylamine as a model molecule for a secondary amine, thermodynamic and kinetic parameters have been calculated for all the elementary reactions in THF as shown in Scheme 1 and are presented in Table 1. The values in the gas phase are presented in Table S1 in the Supporting Information.

Amine assistance causes a significant decrease in enthalpic barrier, as can be seen from the comparison of reactions **5** and **6** with their unassisted analogues **2** and **4**, respectively. This is

DOI: 10.1021/acs.joc.6b02218
J. Org. Chem. 2016, 81, 12291−12302

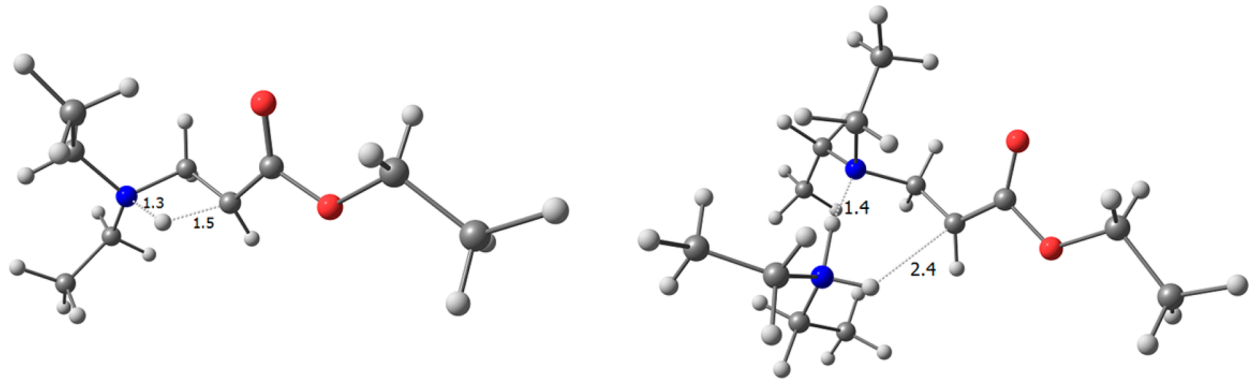

Figure 1. Transition states for the proton transfer from the zwitterionic intermediate (ZI) to the product (**P1**). Left: unassisted (reaction **2**), Right: amine-assisted (reaction **5**).

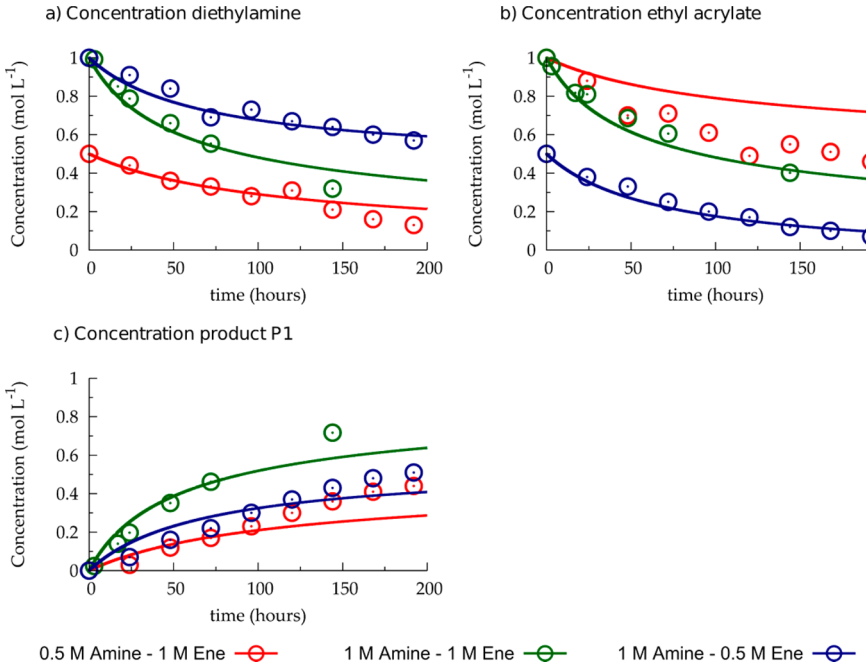

Figure 2. Concentration profiles of diethylamine (a), ethyl acrylate (b), and product **P1** (c) as a function of time for the aza-Michael addition of diethylamine to ethyl acrylate in different conditions. Red: $c_{0,\ amine}$ = 0.5 mol L^{-1}, $c_{0,\ ene}$ = 1 mol L^{-1}; green: $c_{0,\ amine}$ = 1.0 mol L^{-1}, $c_{0,\ ene}$ = 1 mol L^{-1}; blue: $c_{0,\ amine}$ = 1.0 mol L^{-1}, $c_{0,\ ene}$ = 0.5 mol L^{-1}. Lines = simulated data using the microkinetic model and the theoretical parameters, markers = experimental points.

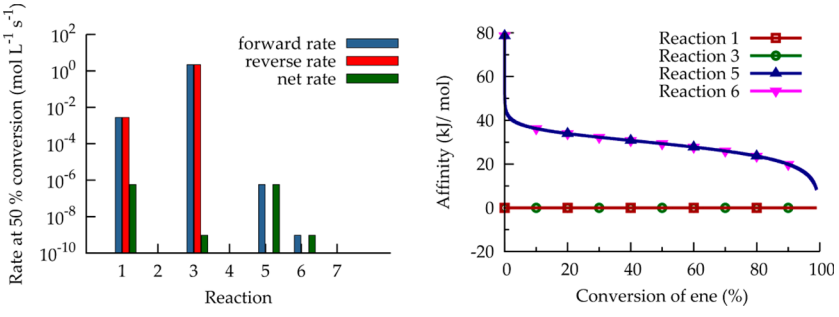

Figure 3. Left: Forward, reverse, and net rates (logarithmic scale) at 50% conversion of all the elementary reactions in the aza-Michael addition of diethylamine to ethyl acrylate as shown in Scheme 1. Right: Thermodynamic affinities of elementary reactions **1**, **3**, **5**, and **6** as a function of the conversion of the ene in the aza-Michael addition of diethylamine to ethyl acrylate. $c_{0,\ amine}$ = 1.0 mol L^{-1}, $c_{0,\ ene}$ = 1 mol L^{-1}.

because the proton transfer reaction can take place over an advantageous six membered ring structure,[43] as shown in Figure 1 for the transition states of reaction **2** and **5** (cf. Figure S9 in the Supporting Information for reactions **4** and **6**). Despite the fact that there is also a larger loss in entropy, i.e., mainly the loss of rotational and translational entropy of the assisting amine, this, nevertheless, does lead to a lowered Gibbs free energy barrier and thus a higher rate coefficient. Note that this is not the case for the

DOI: 10.1021/acs.joc.6b02218
J. Org. Chem. 2016, 81, 12291−12302

proton transfer involved in enol formation (reaction 7): assistance by the amine now occurs through an eight membered ring structure, which is enthalpically not significantly more advantageous than the six membered ring in the unassisted analogue, reaction **3** (cf. Figure S10 in the Supporting Information). The larger loss in entropy now causes a higher Gibbs free energy barrier.

Next, the calculated rate coefficients (Table 1) were used in a microkinetic model to simulate the forward and reverse rate for all the elementary steps considered in Scheme 1. Conversion profiles were simulated at the same conditions as for the performed experiments and are presented in Figure 2 together with the experimental data. Note that the theoretical values were used in the kinetic model without any alteration, demonstrating the accuracy of the used methods for this system.

In order to obtain more insight into the reaction mechanism, the forward, reverse, and net rates of all the elementary steps of the reaction mechanism can be analyzed. These are shown in Figure 3 (left) at 50% conversion.

The dominant reaction mechanism can be determined readily via analysis of the net rates of the elementary steps. Clearly, the operative reaction mechanism consists of (i) the formation of a zwitterionic intermediate (**1**) followed by (ii) the proton transfer assisted by another amine molecule (**5**). This mechanism corresponds to the 1,2-nucleophilic addition. The forward and reverse rates for elementary steps **1** and **3** are very high and almost equal, indicating that these reactions are quasi-equilibrated. This is reflected by the thermodynamic affinity,[44] shown in Figure 3 (right), which is zero for elementary steps **1** and **3**.

Elementary steps **5** and **6** can be considered to go mainly forward because their reverse rate is not significant, as is illustrated further by their thermodynamic affinities which, being significantly larger than zero, show a major driving force toward the product side. Elementary step **5** is therefore the rate controlling step in the dominant mechanism, and, because it is an amine-assisted reaction, the global reaction becomes thus second order in terms of the amine concentration. This is in correspondence with an earlier experimental kinetic study on aza-Michael additions by Popov et al.[40] in another aprotic polar solvent: acetonitrile. Note that in polar protic solvents, this might be very different, since in that scenario a solvent molecule can take over the assisting role. This has been investigated for water as a solvent in a study by Pardo et al.[41]

It is known that for catalyzed aza-Michael additions to certain compounds, such as the base catalyzed addition to chalcones[45] or the gold catalyzed addition to cyclohexenone,[46] the reverse reaction is possible: the retro aza-Michael reaction. The presented reaction analysis shows clearly that this is unlikely for the uncatalyzed aza-Michael addition to ethyl acrylate (and derivatives, as shown further) under the discussed reaction conditions, as even at very high conversions (>90%), there is still a significant thermodynamic driving force toward the products.

Note that the path to the formation of the enol intermediate (**3**), corresponding to the 1,4-nucleophilic addition has a much lower free energy barrier (cf. Table 1). This can be rationalized by the hydrogen bond which is already present along this reaction coordinate (cf. Figure S11 in the Supporting Information). In the ab initio study by Pardo et al.,[41] a similar preference for the 1,4-nucleophilic addition was advocated. However, since the barrier for the subsequent tautomerization via an amine-assisted proton transfer between the enol intermediate and the keto product (**6**) is significantly higher than the barrier for 1,2-addition (**5**), the contribution of the 1,4-addition followed by keto−enol tautomerization is kinetically not significant (cf. Figure 3) and conversion can be assumed to almost exclusively take place via the 1,2-addition. This is also illustrated in a Gibbs free energy diagram in Figure 4.

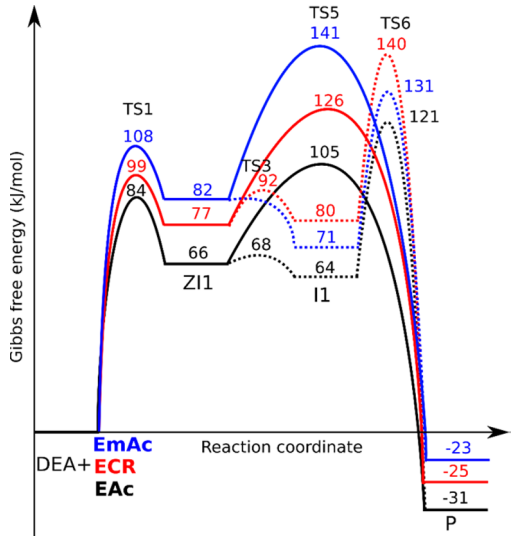

Figure 4. Comparison of the standard Gibbs free energy profile at 298.15 K for the amine-assisted 1,2-addition (full lines, elementary reactions **1**−**5** in Scheme 1) and the 1,4-addition followed by direct keto−enol tautomerization (dotted lines; elementary reactions **1**−**3**−**6** in Scheme 1). The aza-Michael addition of diethylamine to ethyl acrylate is shown in black, to ethyl crotonate in red, and to ethyl methacrylate in blue. For clarity only the lowest energy diastereomers are shown.

Note, however, that the relative contributions of both paths can be expected to depend on the type of solvent used. In addition, nonassisted intramolecular keto−enol tautomerization (**4**) is unlikely as the Gibbs free energy barrier is very high (213.6 kJ/mol at 298.15 K). This high value is in agreement with other computational results obtained for unassisted keto−enol conversions.[47]

To analyze the effects of alkyl substituents on the double bond on the preferred reaction path, the aza-Michael addition of diethylamine to ethyl methacrylate and to ethyl crotonate was investigated (see Scheme 2).

Scheme 2. Ethyl Crotonate (ECR, Left) and Ethyl Methacrylate (EmAc, Right)

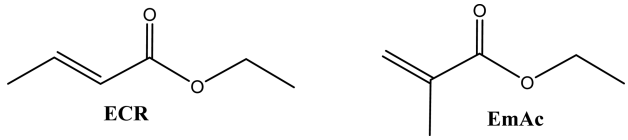

The Gibbs free energy diagram at 298.15 K in THF for the two competing paths, the amine-assisted 1,2-nucleophilic addition (**5**), and the 1,4-nucleophilic addition followed by an amine-assisted tautomeric proton transfer (**3** and **6**) are shown for ethyl crotonate and ethyl methacrylate in Figure 4. The first step, i.e., the formation of the zwitterionic intermediate, is for both methyl-substituted acrylate derivatives more endergonic and with a higher activation Gibbs free energy than for ethyl acrylate. This can be rationalized both in terms of increased steric

DOI: 10.1021/acs.joc.6b02218
J. Org. Chem. 2016, 81, 12291−12302

Scheme 3. Reaction Network for the Aza-Michael Addition of Ethylamine to Ethyl Acrylate in an Aprotic Solvent[a]

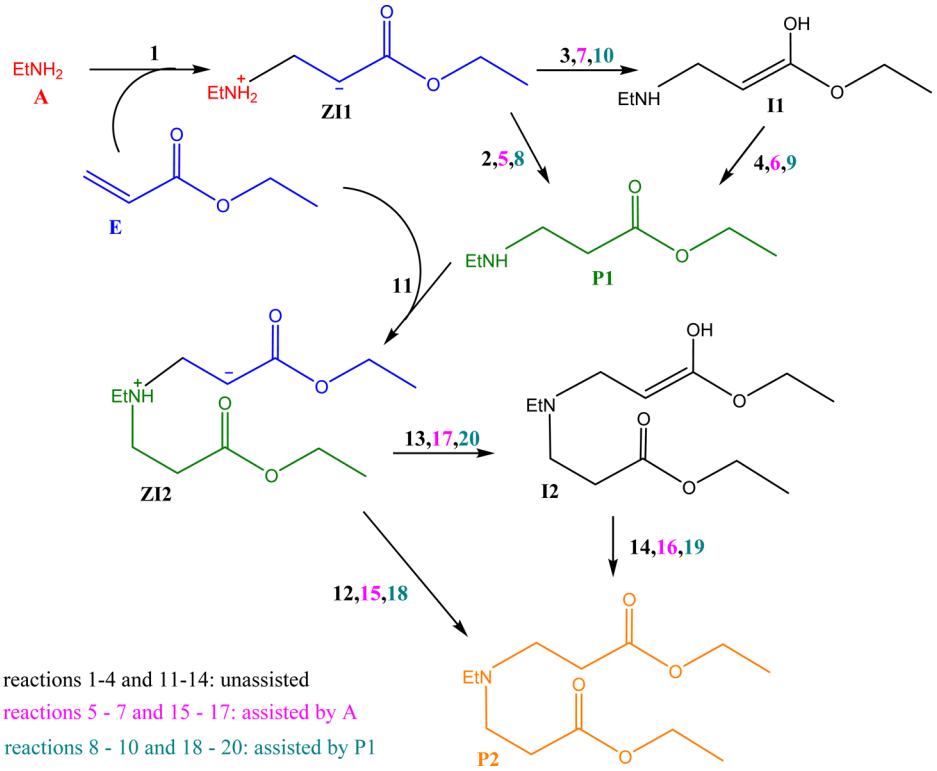

[a]Different reactions involving the same reactants and products are grouped under one arrow to make the scheme more clear. As indicated; reactions **1** − **4** and **11**−**14** are unassisted, reactions **5** − **7** and **15** − **17** are assisted reactions involving the reactant amine (**A**) and reactions **8** − **10** and **18** − **20** are assisted reactions involving the single substituted product amine **P1**.

hindrance as well as the electron donating effect of the extra methyl substituent.

For ethyl crotonate, the subsequent proton transfers appear to be more or less similar as to acrylates and the 1,2-addition remains the most favored reaction path. For methacrylates, on the other hand, the path corresponding to the 1,4-addition (**5**) becomes comparatively more activated and the path corresponding to the 1,2-addition followed by an amine-assisted tautomeric proton transfer becomes the more favored one. However, for both ethyl crotonate and ethyl methacrylate, the corresponding rate coefficients become very low (cf. Table S2 in the Supporting Information) and kinetic simulations predict that virtually no conversion takes place at the given conditions.

Aza-Michael Addition with a Primary Amine. The aza-Michael addition of primary amines to acrylates is quite similar as for secondary amines, but becomes more complicated due to the fact that the aza-Michael adduct (**P1**) is now a secondary amine which can compete with the reactant, the primary amine, for the available acrylates. The complete reaction scheme is shown in Scheme 3. This leads to the formation of a double substituted product, **P2**, as has been shown experimentally before, e.g., in a study by Medina et al.[34]

Additionally, all possible proton transfers can be assisted by either the primary amine reactant (reactions **5**, **6**, 7, and **15**, **16**, **17**), or by the secondary amine product **P1** (reactions **8**, **9**, **10**, and **18**, **19**, **20**).

Standard reaction enthalpies, entropies, and Gibbs free energies and activation enthalpies, entropies, and Gibbs free energies were calculated at 298.15 K in THF for the reaction of ethylamine with ethyl acrylate and are shown in Table 2. The corresponding values in gas phase can be found in Table S4 in the Supporting Information. It is important to notice that in the amine-assisted transition states chiral centers arise, since the transition bonds being formed make the nitrogen of the assisting amine quaternary, and therefore it cannot longer undergo inversion. This is illustrated in Scheme 4 for **TS5**: the transition state from **ZI1** to **P1**. Note that when the substituents R1 and R2 on the amine are equal (as in the case of diethylamine) only 1 chiral center remains.

However, in the case of ethylamine, this is not the case and several distinct diastereoisomers for the transition states can be located, as shown for TS5 in Figure 5 for the SSR and the SRR diastereomers.

All other diastereomeric transition state structures along the dominant path are shown in Section S5.3 in the Supporting Information. The kinetic parameters corresponding to the different diastereomoric transition states are, of course, also different depending on the configuration of their stereocenters, as explicitly indicated in Table 2.

Note that for the elementary steps that are not on the dominant path, only the lowest energy diastereomer was calculated to facilitate the computational workload. The corresponding rate coefficients were used as an upper limit for the rate coefficients corresponding to the other diastereomeric transition states of that elementary step since their contribution to the total reaction is found to be insignificant.

The formation of the first zwitterion (**ZI1**) has a lower reaction enthalpy and a slightly lower reaction Gibbs free energy for the primary amine than for diethylamine in THF (62.0 vs 66.4 kJ mol^{-1}, respectively). This might seem to contradict the well-known fact that secondary amines are stronger nucleophiles than primary amines, which is true in water and also in the gas phase

DOI: 10.1021/acs.joc.6b02218
J. Org. Chem. 2016, 81, 12291−12302

Table 2. Standard Reaction Enthalpy, Entropy, and Gibbs Free Energy[a]; Standard Activation Enthalpy, Entropy, and Gibbs Free Energy[b]; and Forward and Reverse Rate Coefficients (in L mol^{-1} s^{-1} or s^{-1}) at 298.15 K in THF for All Elementary Reactions in the Reaction Network of the Aza-Michael Addition of Ethylamine to Ethyl Acrylate[c]

reaction	diastereomer TS	$\Delta_rH°$	$\Delta_rS°$	$\Delta_rG°$	$\Delta^‡H°$	$\Delta^‡S°$	$\Delta^‡G°$
R1		22.5	−160.9	70.4	32.8	−152.7	91.5
R2		−88.7	44.9	−102.1	93.0	34.9	87.8
R3		4.5	31.1	−4.8	−1.5	3.5	2.4
R4		−93.2	13.8	−97.3	218.4	6.1	213.5
R5	RRS	−88.7	44.9	−102.1	−4.5	−97.7	29.8
	RSS				−9.6	−101.9	25.9
R6	RR	−93.2	13.8	−97.3	0.7	−147.9	39.6
	RS				0.8	−142.0	38.0
R7		4.5	31.1	−4.8	−30.8	−97.9	4.8
R8	RRS	−88.7	44.9	−102.1	9.6	−82.7	38.3
	RSS				8.3	−73.0	34.1
R9		−93.2	13.8	−97.3	24.1	−114.0	52.9
R10		4.5	31.1	−4.8	−25.8	−102.1	9.4
R11		36.7	−137.4	77.7	41.3	−137.2	92.9
R12		−99.8	14.4	−104.1	78.6	−2.1	85.0
R13		−9.6	−5.9	−7.9	−10.6	−14.7	−2.1
R14		−90.2	20.4	−96.3	218.5	−12.7	218.9
R15	RRR	−99.8	14.4	−104.1	−24.3	−138.9	27.3
	RRS				−17.7	−134.9	32.7
	RSR				−21.9	−136.0	28.8
	RSS				−17.8	−139.9	34.0
TS16	RR	−90.2	20.4	−96.3	0.6	−145.8	42.1
	RS				−6.2	−145.6	35.3
R17		−9.6	−5.9	−7.9	−28.7	−114.8	12.3
R18	RRR	−99.8	14.4	−104.1	−11.3	−132.3	37.6
	RRS				−9.6	−135.2	40.3
	RSR				−9.9	−142.5	42.0
	RSS				−13.3	−181.7	50.4
R19		−90.2	20.4	−96.3	11.9	−124.5	58.3
R20		−9.6	−5.9	−7.9	−3.2	−148.1	41.7

[a] $\Delta_rH°$, $\Delta_rS°$, $\Delta_rG°$, in respectively kJ mol^{-1}, J mol^{-1} K^{-1}, kJ mol^{-1}. [b] $\Delta^‡H°$, $\Delta^‡S°$, $\Delta^‡G°$, in respectively kJ mol^{-1}, J mol^{-1} K^{-1}, kJ mol^{-1}. [c] As shown in Scheme 3. Values for different diastereomeric transition states are shown if applicable.

Scheme 4. Illustration of the Chiral Centers Arising in an Assisted Transition State, Such as TS5

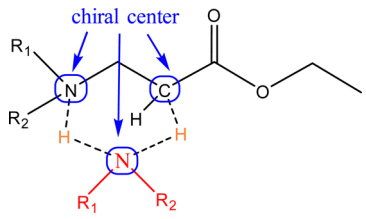

(97.4 vs 87.7 kJ mol^{-1}, respectively, cf. Tables S1 and S4 in the Supporting Information); however, these relations cannot simply be transferred to other solvents.[48] This is because the zwitterionic intermediate (**ZI1**) is relatively more solvated in THF in the case of primary amines than in the case of secondary amines (35.4 vs 21.3 kJ mol^{-1}), due to the fact that the positive charge is more pronounced and better accessible for the partially negatively charged oxygens of the THF solvent molecules. This is qualitatively illustrated via visualization of the surface charges in Figure 6.

Taking into account the different stereoisomers, rate coefficients for all the forward and reverse elementary steps were calculated and are shown in Table 3. Clearly, proton transfer reactions assisted by a primary amine are significantly faster than equivalent proton transfer reactions assisted by a secondary amine. It was therefore decided to account for possible diffusional limitations for the bimolecular reactions with intrinsic rate coefficients faster than 10^8 mol L^{-1} s^{-1} (**5**, **8**, **10**, **15**, and **17**). This was done by the introduction of an apparent rate coefficient according to the coupled encounter pair model using mutual diffusivity coefficients that were calculated from molecular dynamics simulations.

The apparent rate coefficients from Table 3 are used in a microkinetic model to simulate the aza Michael-addition of *n*-octylamine to ethyl acrylate. Concentrations profiles of the reactants (**A** and **E**) and the two formed products (**P1** and **P2**) are shown in Figure 7. Note that *n*-octylamine is used for the experiments, since lighter amines are found to slowly evaporate from the reaction mixture. The use of smaller alkyl groups as a model for larger ones is well-justified as it was found to be of little influence for similar reactions[49] as long as this does not cause steric hindrance (cf. also Section S5.1 in the Supporting Information). Again, an excellent agreement between theory and experiment is found.

To determine the operative reaction mechanism, the net rates of the elementary steps were analyzed as shown in Figure 8.

Formation of the single substituted product **P1** occurs predominantly via 1,2-addition involving the formation of a zwitterion (**1**) followed by a primary amine-assisted 1,2-

DOI: 10.1021/acs.joc.6b02218
J. Org. Chem. 2016, 81, 12291−12302

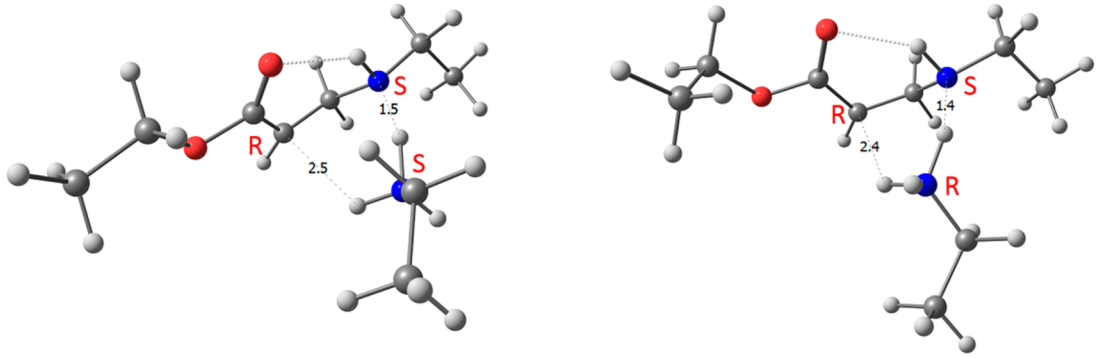

Figure 5. SSR (left) and SRR (right) diastereomers of **TS5**. The RRS and RSS diastereomers are the respective mirror images and have the same kinetic parameters. Diastereomers RRR−SSS and RSR−SRS are not included as they do not have a stabilizing H-bridge and are, as such, significantly higher in energy.

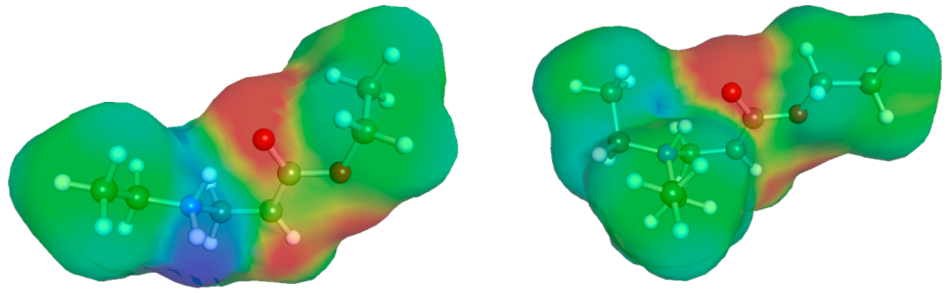

Figure 6. Surface charge distribution on the zwitterionic intermediate (**ZI1**) in the case of the aza-Michael addition of ethylamine (left) or diethylamine (right) to ethyl acrylate. Red corresponds to a negative surface charge, blue to a positive surface charge.

Table 3. Equilibrium Coefficients (in L mol^{-1} or Dimensionless), Chemical Forward and Reverse Rate Coefficients (in L mol^{-1} s^{-1} or s^{-1}), Diffusional Limitations (in L mol^{-1} s^{-1}), and Apparent Forward and Reverse Rate Coefficients (in L mol^{-1} s^{-1} or s^{-1}) at 298.15 K in THF for All Elementary Reactions in the Reaction Network of the Aza-Michael Addition of Ethylamine to Ethyl Acrylate, As Shown in Scheme 3

reaction	K	k_+	k_-	k_{diff}	$k_{app,+}$	$k_{app,-}$
R1	4.5×10^{-13}	1.1×10^{-03}	2.5×10^{09}		1.1×10^{-03}	2.5×10^{09}
R2	8.1×10^{17}	5.2×10^{-03}	6.4×10^{-21}		5.2×10^{-03}	6.4×10^{-21}
R3	6.9×10^{00}	4.8×10^{12}	6.9×10^{11}		4.8×10^{12}	6.9×10^{11}
R4	1.2×10^{17}	4.9×10^{-25}	4.2×10^{-42}		4.9×10^{-25}	4.2×10^{-42}
R5	8.1×10^{17}	4.6×10^{08}	5.7×10^{-10}	1.9×10^{09}	3.7×10^{08}	4.6×10^{-10}
R6	1.2×10^{17}	4.3×10^{06}	3.7×10^{-11}		4.3×10^{06}	3.7×10^{-11}
R7	6.9×10^{00}	3.7×10^{12}	5.3×10^{11}	1.4×10^{09}	1.4×10^{09}	2.0×10^{08}
R8	8.1×10^{17}	1.6×10^{07}	2.0×10^{-11}		1.6×10^{07}	2.0×10^{-11}
R9	1.2×10^{17}	1.4×10^{04}	1.2×10^{-13}		1.4×10^{04}	1.2×10^{-13}
R10	6.9×10^{00}	5.7×10^{11}	8.2×10^{10}	1.3×10^{09}	1.3×10^{09}	1.8×10^{08}
R11	2.5×10^{-14}	6.8×10^{-04}	2.7×10^{10}		6.8×10^{-04}	2.7×10^{10}
R12	1.8×10^{18}	1.6×10^{-02}	9.1×10^{-21}		1.6×10^{-02}	9.1×10^{-21}
R13	2.3×10^{01}	1.2×10^{13}	5.3×10^{11}		1.2×10^{13}	5.3×10^{11}
R14	7.7×10^{16}	5.5×10^{-26}	7.2×10^{-43}		5.5×10^{-26}	7.2×10^{-43}
R15	1.8×10^{18}	3.6×10^{08}	2.0×10^{-10}	1.4×10^{09}	2.9×10^{08}	1.6×10^{-10}
R16	7.7×10^{16}	9.0×10^{06}	1.2×10^{-10}		9.0×10^{06}	1.2×10^{-10}
R17	2.3×10^{01}	2.5×10^{13}	1.1×10^{12}	1.2×10^{09}	1.2×10^{09}	5.2×10^{07}
R18	1.8×10^{18}	4.9×10^{06}	2.7×10^{-12}		4.9×10^{06}	2.7×10^{-12}
R19	7.7×10^{16}	1.6×10^{03}	2.1×10^{-14}		1.6×10^{03}	2.1×10^{-14}
R20	2.3×10^{01}	1.2×10^{06}	5.2×10^{04}		1.2×10^{06}	5.2×10^{04}

nucleophilic addition (**5**). Toward the end of the reaction, also assistance by the secondary amine (**P1**) starts to play a role (**8**). However, 1,4-nucleophilic addition followed by amine-assisted keto−enol tautomerization cannot be completely excluded, since the contribution from reaction **6** cannot be ignored. The same reasoning is applicable to the formation of the double substituted product **P2**. Here the contribution of the 1,4-nucleophilic addition followed by primary amine-assisted keto−enol tautomerism (**16**) is even more important. To further quantify the importance of the individual elementary steps, relative contributions of each path have been determined for the formation of both products, **P1** and **P2** and are shown in Figure

DOI: 10.1021/acs.joc.6b02218
J. Org. Chem. 2016, 81, 12291−12302

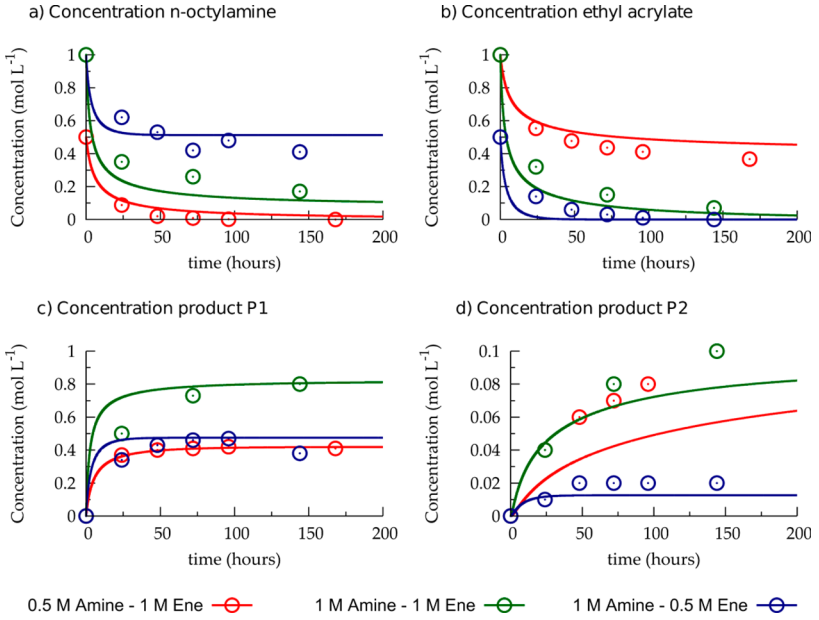

Figure 7. Concentration profiles of *n*-octylamine (a), ethyl acrylate (b), product **P1** (c), and product **P2** (d) as a function of time for the aza-Michael addition of *n*-octylamine to ethyl acrylate in different conditions. Red: $c_{0,\ amine}$ = 0.5 mol L^{-1}, $c_{0,\ ene}$ = 1 mol L^{-1}; green: $c_{0,\ amine}$ = 1.0 mol L^{-1}, $c_{0,\ ene}$ = 1 mol L^{-1}; blue: $c_{0,\ amine}$ = 1.0 mol L^{-1}, $c_{0,\ ene}$ = 0.5 mol L^{-1}. Lines = simulated data using the microkinetic model and the apparent rate coefficients from Table 3, markers= experimental points.

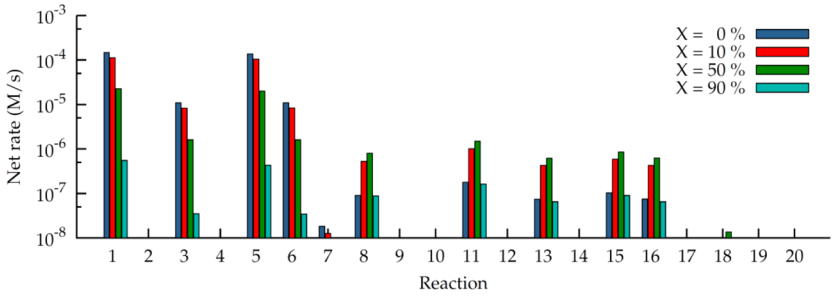

Figure 8. Net rates (logarithmic scale) at different conversion (X) levels (0% blue, 10% red, 50% green, and 90% cyan) of all elementary reactions in the aza-Michael addition of *n*-octylamine to ethyl acrylate as shown in Scheme 3 and using the apparent rate coefficients from Table 3. $c_{0,\ amine}$ = 1.0 mol L^{-1}, $c_{0,\ ene}$ = 1 mol L^{-1}.

9. Especially for the formation of **P2**, the contribution of the alternative path (**1**−**3**−**6**) is significant.

Thermodynamic affinities are shown in Figure S18 in the Supporting Information, and are similar to the ones obtained for the aza-Michael addition of secondary amines (Figure 3, right). In the case of the 1,4-nucleophilic addition, the formation of the zwitterionic intermediates, **ZI1** (**1**) and **ZI2** (**11**) is quasi-equilibrated while the subsequent proton transfer (**5** or **8** and **15** or **18**, respectively) controls the rate. Note that reactions **5** and **15** are limited by diffusion. For the alternative path corresponding to the 1,2-nucleophilic addition followed by keto−enol tautomerization, also the internal proton transfer between the zwitterionic intermediate and the enolic intermediate (**3** or **13**) is pseudoequilibrated, while the subsequent keto−enol tautomerization (**6** or **16**) is rate controlling.

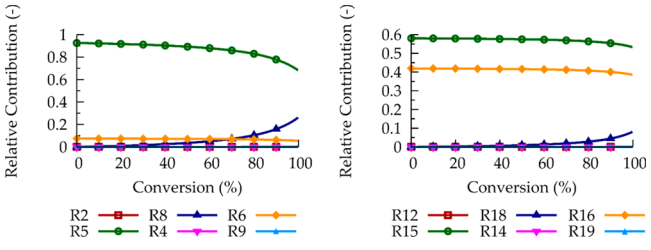

Figure 9. Relative contributions to the formation of the single substituted product **P1** (left) and of the double substituted product **P2** (right) as a function of the conversion for the aza-Michael addition of *n*-octylamine to ethyl acrylate in THF at 298.15 K using the parameters from Table 3. The numbers of the reactions (R#) correspond to Scheme 1. $c_{0,\ amine}$ = 1.0 mol L^{-1}, $c_{0,\ ene}$ = 1 mol L^{-1}.

The relative contribution of the 1,4-nucleophilic addition to the total reaction can be rationalized by analyzing the Gibbs free energy diagram as shown in Figure 10. Compared to the Gibbs free energy diagram of diethylamine to ethyl acrylate the steps involving the amine-assisted keto−enol tautomerism (**6** and **16**) for ethylamine have a relatively lower barrier, probably due to less steric hindrance. Comparing the aza-Michael addition to ethyl acrylate in an aprotic solvent of primary amines with secondary amines, the latter is occurring slower, as for similar reaction times, conversions are lower. This might seem counterintuitive, since secondary amines are known to be more nucleophilic and would therefore be expected to be more reactive.[3] The reason for this is the amine-assisted proton transfer, which occurs more

DOI: 10.1021/acs.joc.6b02218
J. Org. Chem. 2016, 81, 12291−12302

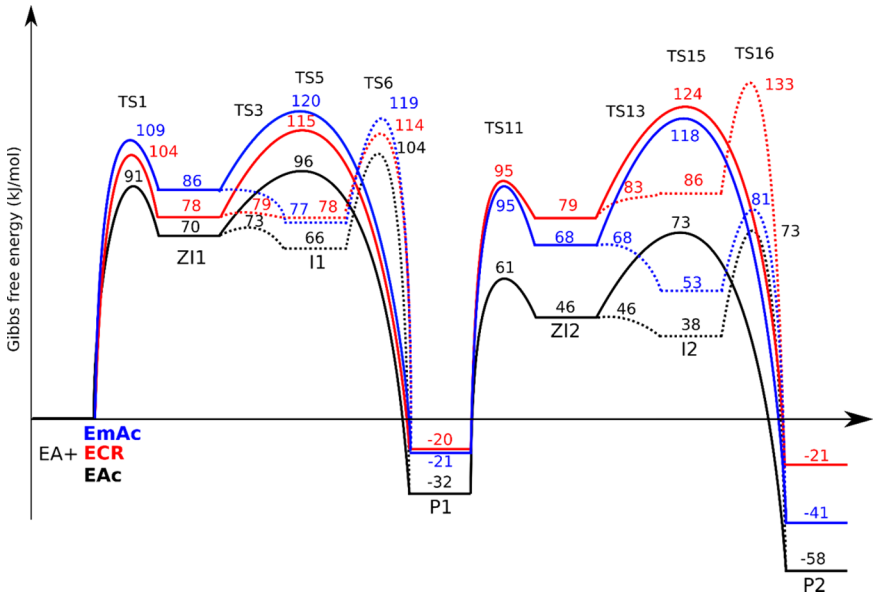

Figure 10. Standard Gibbs free energy of formation at 298.15 K of the stationary points (lowest energy conformers only) along the two reaction paths in the double aza-Michael addition of ethylamine to ethyl acrylate (black), ethyl crotonate (red), and ethyl methacrylate (blue): the 1,2-addition (elementary reactions **1**−**5** and **11**−**15**) and the 1,4-addition followed by keto−enol tautomerism (elementary reactions **1**−**3**−**6** and **11**−**13**−**16**). Labels are according to Scheme 3.

easily with ethylamine as it is less sterically hindered. In the case of ethylamine, these proton transfer reactions are so fast that diffusional limitations become important.

Similarly to diethylamine, also the aza-Michael addition of ethylamine to the acrylate derivatives, ethyl crotonate and ethyl methacrylate, becomes significantly more activated and thus slower when compared to the reaction with ethyl acrylate (Figure 10). This agrees with the experimental study from Medina et al.,[34] where the aza-Michael addition to crotonates did not yield any product at ambient conditions. For both acrylate derivatives, both the primary-amine-assisted 1,2-nucleophilic addition (**5**) and the 1,4-nucleophilic addition (**3**) followed by amine-assisted keto−enol tautomerization (**6**) contribute to the formation of the first Michael adduct **P1**, since the total energy barriers have similar values (for ethyl crotonate 115 vs 114 kJ mol^{-1}, for ethyl methacrylate 120 vs 119 kJ mol^{-1}, respectively). For the second addition (of **P1** + **E** to **P2**), the 1,2-addition is the favored mechanism for the addition to ethyl crotonate, while the 1,4-addition followed by keto−enol tautomerization becomes the favored mechanism for the addition to ethyl methacrylate (see Figures S19 and S20 in the Supporting Information for relative contributions). This follows the same trend as for the aza-Michael addition using diethylamine.

3. CONCLUSIONS

A kinetic model of the aza Michael addition of primary and secondary amines to ethyl acrylate in THF is constructed based on a detailed reaction scheme. Using advanced computational methods, accurate rate coefficients for all elementary steps were calculated and used to simulate conversion profiles in excellent agreement with experimental data. It is shown that for primary amines the aza-Michael addition involves a 1,2-addition occurring via the pseudoequilibrated formation of a zwitterionic intermediate followed by a diffusion controlled amine-assisted proton transfer toward the keto-product. Contributions from an alternative path, involving a 1,4-addition which consists of the formation of an enolic intermediate followed by amine assisted keto−enol tautomerization, remain limited. The formed singly substituted aza-adduct, being a secondary amine, successfully competes for the ene with the primary amine to form the doubly substituted adduct. This reaction mechanism occurs mainly via a similar 1,2-addition mechanism, but also via a 1,4-addition followed by a direct keto−enol tautomerization assisted by a primary amine.

In the case of the aza-Michael addition of secondary amines, a similar 1,2-addition mechanism is operative and the 1,4-addition path can now be neglected because the subsequent keto−enol tautomerization being assisted by a secondary amine becomes too high in activation energy. In contrast to what is observed in water, in THF secondary amines react slower than primary amines. The reason for this is twofold: (i) the amine assisted proton transfer reactions experience more steric hindrance in the case of secondary amines and (ii) the zwitterionic intermediate formed in the first step is solvated to a lesser extent, which is related to the less pronounced positive charge and the decreased accessibility for the THF oxygen. Furthermore, the relative contributions of 1,2- and 1,4-addition are significantly influenced by the presence of alkyl substituents on the double bond. For methacrylates the 1,4-addition path even becomes the dominant route for the aza-Michael addition with secondary amines. However, the presence of these alkyl substituents also considerably increases the reaction barrier, which becomes too high for the reaction to take place at room temperature.

4. METHODS

Experimental Details. Diethylamine, *n*-octylamine, ethyl acrylate, decane, tetrahydrofuran (THF) were used as received. The experiments were performed according to the reaction conditions specified in Table 4.

The example for a typical example is given for the case of entry 2 in Table 4: A two-neck flask of 50 mL was filled with 28.6 mL THF, 1.9 mL decane, and 4.2 mL of ethyl acrylate and sealed with rubber septums. The flask was placed in a water bath which was kept at a constant temperature of 25 °C. Upon addition of 4 mL of diethylamine the reaction was started. Samples of approximately 0.1 mL were taken at

DOI: 10.1021/acs.joc.6b02218
J. Org. Chem. 2016, 81, 12291−12302

Table 4. Details for the Aza-Michael Additions Performed with Ethyl Acrylate in THF at Room Temperature

entry	amine	c_{amine} (M)	c_{ene} (M)	volume (mL)
1	diethylamine	0.5	1.0	38.7
2	diethylamine	1.0	1.0	38.7
3	diethylamine	1.0	0.5	38.7
4	*n*-octylamine	0.5	1.0	19.0
5	*n*-octylamine	1.0	1.0	24.2
6	*n*-octylamine	1.0	0.5	26.0

fixed time intervals and their composition was determined immediately using gas chromatography (GC). A full description of the GC analysis procedure is given in section S1 in the Supporting Information.

Computational Details. The Gaussian-09 package[50] was used for all electronic structure calculations. Global minimum energy conformations for reactants, products, and intermediates are determined by rotating all dihedral angles at the B3LYP/6-31G(d) level of theory, using the SMD universal solvation model from Marenich, Kramer, and Truhlar,[51] using the parameters for THF (ε_r= 7.4257). Transition states were located and optimized using the Berny algorithm,[52] and, where possible, also the different conformations were scanned. All minimum energy conformations and transition states are confirmed to have zero and one imaginary frequency, respectively.

As chemical accuracy is desired due to the need of the data to be quantitatively used in a microkinetic model, the composite method CBS-QB3 was envisioned for the calculation of the electronic energies. However, the size of the molecules made this computationally impossible. Therefore, it was opted to use an ONIOM-based scheme,[53,54] partitioned into a high level using CBS-QB3, and a low level using the M06-2X functional from Zhao and Truhlar[55] with a large split-valence triple-ζ polarized basis set, enlarged with a diffuse function, 6-311+G(d,p), as this functional is reported to provide reliable energetics for a similar chemical system.[56] A full description of the partitioning of all the chemical species is given in Section S2 in the Supporting Information.

Thermal contributions were calculated in the quasiharmonic oscillator approach[57] at the B3LYP/6-31G(d) level of theory, meaning that all frequencies smaller than 30 cm^{-1} were set at 30 cm^{-1}, in order to correct for the failure of the harmonic oscillator model at low-frequency vibrations. Furthermore, a recommended scaling factor of 0.99, as determined by Scott and Radom[58] was applied. The standard thermodynamic formulas[59] were then used to obtain standard enthalpies, entropies, and Gibbs free energies in gas phase (eqs 1−3):

$$H^\circ_{gas} = E + RT^2\left(\frac{\partial \ln q}{\partial T}\right)_V + PV \tag{1}$$

$$S^\circ_{gas} = R + R\ln(q(V,T)) + RT\left(\frac{\partial \ln q}{\partial T}\right)_V \tag{2}$$

$$G^\circ_{gas} = H^\circ_{gas} - TS^\circ_{gas} \tag{3}$$

Where E is the electronic energy calculated using ONIOM, P the pressure equal to 1 atm, V the volume equal to 1 L, R the universal gas constant, T the temperature equal to 298.15 K, and q the total partition function including the contribution due to the zero-point energy vibration at the B3LYP/6-31G(d) level of theory.

Standard Gibbs free energies of solvation in THF, $\Delta_{solv}G^\circ(T)$, were calculated using COSMO-RS[60] theory as implemented in the COSMOtherm[61] software, version C30_1601, based on BP86/TZVP calculations on the B3LYP/6-31G(d)//SMD(THF) optimized structures, as this is the level of theory to which COSMO-RS is parametrized. Standard enthalpies and entropies of solvation were then calculated by using the following thermodynamic functions. These numbers were then added to their respective values in the gas phase to obtain the value in THF (eqs 4 and 5).

$$\Delta_{solv}H^\circ(T) = -T^2\frac{\partial\left(\frac{\Delta_{solv}G^\circ(T)}{T}\right)}{\partial T} \approx -T^2\frac{\left(\frac{\Delta_{solv}G^\circ(T_2)}{T_2}\right) - \left(\frac{\Delta_{solv}G^\circ(T_1)}{T_1}\right)}{T_2} \tag{4}$$

$$\Delta_{solv}S^\circ(T) = \frac{\Delta_{solv}H^\circ(T) - \Delta_{solv}G^\circ(T)}{T} \tag{5}$$

Forward and reverse rate coefficients in THF, k_+ and k_-, were then calculated based on the ab initio determined Gibbs free energy in THF using classical transition state theory:[59] The contribution of all the diastomeric transition states, arising through the formation of chiral centers as shown in Scheme 4, are explicitly taken into account (eqs 6−8).

$$k_+ = \sum_j n_j \frac{k_B T}{h} e^{-\Delta^\ddagger G^\circ_j/RT} \tag{6}$$

$$K = e^{-\Delta_r G^\circ/RT} \tag{7}$$

$$k_- = \frac{k_+}{K} \tag{8}$$

Where n_j is the reaction degeneracy corresponding to the diastereomeric transition state j, k_B is the Boltzmann constant, h the Planck constant, $\Delta^\ddagger G^\circ_j$ is the difference in standard Gibbs free energy between the transition state j and the reactant(s), and $\Delta_r G^\circ$ the difference in standard Gibbs free energy between the product and the reactant(s). Note that, instead of making the summation of the different reaction paths corresponding to the transition state diastereomers, it is mathematically equivalent to consider one transition state with a free energy equal to the Boltzmann average of the free energies of all diastereomers.

For bimolecular reactions having an intrinsic chemical rate coefficient higher than 10^8 mol L^{-1} s^{-1}, such as proton transfer reactions, diffusional effects can no longer be ignored and were thus accounted for using the coupled encounter pair model.[62−64] This leads to the following expressions for the apparent rate coefficients (eqs 9 and 10):

$$\frac{1}{k_{app,+}} = \frac{1}{k_+} + \frac{1}{k_{diff}} \tag{9}$$

$$\frac{1}{k_{app,-}} = \frac{1}{k_-} + \frac{K}{k_{diff}} \tag{10}$$

The diffusional contribution k_{diff} was calculated using the Smoluchowski model[65] (eq 11):

$$k_{diff} = 4\pi N_A \sigma D_{ij} \tag{11}$$

Where σ is the reaction distance and D_{ij} the mutual diffusivity coefficient of i toward j, calculated in THF using the diffusion coefficients of the reactants in THF and the self-diffusion coefficient of THF in THF,[66] according to eq 12:[66]

$$D_{ij} = \frac{D_{i,THF}D_{j,THF}}{D_{THF,THF}} \tag{12}$$

Diffusion coefficients can be calculated from the mean square displacement (MSD) of the center of mass of the molecule via the Einstein relation,[67] as shown in eq 13:

$$D_{i,THF} = \frac{1}{6}\lim_{t\to\infty}\frac{d}{dt}\left(\left[\overrightarrow{r(t)} - \overrightarrow{r(0)}\right]^2\right) \tag{13}$$

The MSD of the center of mass, $\left[\overrightarrow{r(t)} - \overrightarrow{r(0)}\right]^2$, was then calculated from classical molecular dynamics simulations, with the MM3 force field[68] using TINKER version 6.2.[69] This was done by simulating an NVT ensemble of the molecule in a cubic box of 8.0 nm^3 (side of 20 Å), filled with THF molecules, for 50 ps at 298.15 K. $D_{i,THF}$ was then

DOI: 10.1021/acs.joc.6b02218
J. Org. Chem. 2016, 81, 12291−12302

calculated using the average of the MSD over the last picosecond. This lead to the diffusion coefficients found in Table 5.

Table 5. Diffusion Coefficients Calculated Using Classical Molecular Dynamics

	diffusion coefficient ($m^2\ s^{-1}$)
THF	2.01×10^{-09}
EA	4.22×10^{-09}
EAc	3.24×10^{-09}
ZI1-EA-EAc	8.45×10^{-10}
P1-EA-EAc	3.05×10^{-09}
ZI2-EA-EAc	5.95×10^{-10}

For the simulation, all elementary reactions were considered, and for each elementary step forward (r_{i+}), reverse (r_{i-}) and net rates (r_i) were calculated as follows (eqs 14–16):

$$r_{i+} = k_{i+} \prod_j c_{i+,j}^{n_{i,j}} \tag{14}$$

$$r_{i-} = k_{i-} \prod_j c_{i-,j}^{n_{i,j}} \tag{15}$$

$$r_i = r_{i+} - r_{i-} \tag{16}$$

Where $c_{i+,j}$ and $c_{i-,j}$ refer to the reactants of respectively the forward and reverse elementary reaction i, and $n_{i,j}$ to their respective stoichiometric coefficients.

Integration of the continuity equations (cf. Section S6 in the Supporting Information) was performed using the LSODA algorithm (i.e., Livermore Solver for Ordinary Equations).[70]

The relative contribution (RC) of an elementary step j to the formation of a product was calculated as shown in eq 17:

$$RC_j = \frac{r_j}{R_P} = \frac{r_j}{\sum_i r_i} \tag{17}$$

Where r_j is the net rate of the considered elementary step and R_P is the net rate of formation of product **P** which is obtained as the summation of the net rates of all the elementary steps i leading to the formation of product **P**. Finally, thermodynamic affinities were calculated using the De Donder relation,[44] shown in eq 18:

$$A = RT \ln \frac{r_+}{r_{r-}} \tag{18}$$

■ ASSOCIATED CONTENT

Supporting Information

The Supporting Information is available free of charge on the ACS Publications website at DOI: 10.1021/acs.joc.6b02218.

Description of the used GC analysis procedure; computational details on the ONIOM-type calculations; an analysis of the possible aminolysis side reaction; extra thermodynamic and kinetic data as well as ball-and-stick representation of transition states and intermediates of the aza-Michael addition of both primary and secondary amines to ethyl acrylate, ethyl methacrylate, and ethyl crotonate; the ordinary differential equations used in the microkinetic model; and Cartesian coordinates of all the stationary points reported in this manuscript, and, in the case of saddle points, with their imaginary frequency (PDF)

■ AUTHOR INFORMATION

Corresponding Author

*E-mail: MarieFrancoise.Reyniers@UGent.be

ORCID

Gilles B. Desmet: 0000-0001-8946-1679
Guy B. Marin: 0000-0002-6733-1213
Filip E. Du Prez: 0000-0003-4065-6373

Notes

The authors declare no competing financial interest.

■ ACKNOWLEDGMENTS

The authors acknowledge financial support from the Long Term Structural Methusalem Funding by the Flemish Government, the Interuniversity Attraction Poles Programme—Belgian State—Belgian Science Policy, and the Fund for Scientific Research Flanders (FWO; G.045212N; G.0065.13N). D.R.D. acknowledges the Fund for Scientific Research Flanders (FWO) through a postdoctoral fellowship. The computational work was carried out using the STEVIN Supercomputer Infrastructure at Ghent University, funded by Ghent University, the Flemish Supercomputer Center (VSC), the Hercules Foundation, and the Flemish Government—department EWI.

■ REFERENCES

(1) Michael, A. *J. Prakt. Chem.* **1887**, *35*, 349.
(2) Michael, A. *J. Am. Chem. Soc.* **1887**, *9*, 112.
(3) Mather, B. D.; Viswanathan, K.; Miller, K. M.; Long, T. E. *Prog. Polym. Sci.* **2006**, *31*, 487.
(4) Yoneda, N.; Hotta, A.; Asano, K.; Matsubara, S. *Org. Lett.* **2014**, *16*, 6264.
(5) Thomas, B. E.; Kollman, P. A. *J. Org. Chem.* **1995**, *60*, 8375.
(6) Hoyle, C. E.; Bowman, C. N. *Angew. Chem., Int. Ed.* **2010**, *49*, 1540.
(7) Nguyen, L.-T. T.; Gokmen, M. T.; Du Prez, F. E. *Polym. Chem.* **2013**, *4*, 5527.
(8) Enders, D.; Saint-Dizier, A.; Lannou, M.-I.; Lenzen, A. *Eur. J. Org. Chem.* **2006**, *2006*, 29.
(9) Zhao, D. P.; Mao, L. J.; Yang, D. X.; Wang, R. *J. Org. Chem.* **2010**, *75*, 6756.
(10) Escalante, J.; Carrillo-Morales, M.; Linzaga, I. *Molecules* **2008**, *13*, 340.
(11) Davies, S. G.; Ichihara, O. *Tetrahedron: Asymmetry* **1991**, *2*, 183.
(12) Bassam, N.; Laure, C.; Jean-Francois, B.; Yann, R.; Zephirin, M. *Green Chem.* **2013**, *15*, 1900.
(13) Wu; Liu, Y.; He; Chung; Goh. *Macromolecules* **2004**, *37*, 6763.
(14) Lynn, D. M.; Langer, R. *J. Am. Chem. Soc.* **2000**, *122*, 10761.
(15) Retailleau, M.; Ibrahim, A.; Croutxé-Barghorn, C.; Allonas, X.; Ley, C.; Le Nouen, D. *ACS Macro Lett.* **2015**, *4*, 1327.
(16) Retailleau, M.; Ibrahim, A.; Croutxe-Barghorn, C.; Allonas, X. *RSC Adv.* **2016**, *6*, 47130.
(17) Read, E. S.; Thompson, K. L.; Armes, S. P. *Polym. Chem.* **2010**, *1*, 221.
(18) Rulev, A. Y. e. *Russ. Chem. Rev.* **2011**, *80*, 197.
(19) Nair, D. P.; Podgorski, M.; Chatani, S.; Gong, T.; Xi, W. X.; Fenoli, C. R.; Bowman, C. N. *Chem. Mater.* **2014**, *26*, 724.
(20) Espeel, P.; Du Prez, F. E. *Eur. Polym. J.* **2015**, *62*, 247.
(21) Espeel, P.; Goethals, F.; Driessen, F.; Nguyen, L.-T. T.; Du Prez, F. E. *Polym. Chem.* **2013**, *4*, 2449.
(22) Espeel, P.; Goethals, F.; Du Prez, F. E. *J. Am. Chem. Soc.* **2011**, *133*, 1678.
(23) Dai, L.; Zhang, Y.; Dou, Q.; Wang, X.; Chen, Y. *Tetrahedron* **2013**, *69*, 1712.
(24) Kantam, M. L.; Laha, S.; Yadav, J.; Jha, S. *Tetrahedron Lett.* **2009**, *50*, 4467.
(25) Verma, S.; Jain, S. L.; Sain, B. *Org. Biomol. Chem.* **2011**, *9*, 2314.
(26) Nath, J.; Chaudhuri, M. K. *Catal. Lett.* **2009**, *133*, 388.
(27) Krishna, P. R.; Sreeshailam, A.; Srinivas, R. *Tetrahedron* **2009**, *65*, 9657.
(28) Xu, L.-W.; Xia, C.-G. *Eur. J. Org. Chem.* **2005**, *2005*, 633.

DOI: 10.1021/acs.joc.6b02218
J. Org. Chem. 2016, 81, 12291–12302

(29) Souza, R. O. M. A. d.; Matos, L. M. C.; Gonçalves, K. M.; Costa, I. C. R.; Babics, I.; Leite, S. G. F.; Oestreicher, E. G.; Antunes, O. A. C. *Tetrahedron Lett.* **2009**, *50*, 2017.
(30) Ranu, B. C.; Banerjee, S. *Tetrahedron Lett.* **2007**, *48*, 141.
(31) Enders, D.; Wang, C.; Liebich, J. X. *Chem. - Eur. J.* **2009**, *15*, 11058.
(32) Sanchez-Rosello, M.; Acena, J. L.; Simon-Fuentes, A.; del Pozo, C. *Chem. Soc. Rev.* **2014**, *43*, 7430.
(33) Wang, J.; Li, P.; Choy, P. Y.; Chan, A. S. C.; Kwong, F. Y. *ChemCatChem* **2012**, *4*, 917.
(34) Medina, F.; Duhal, N.; Michon, C.; Agbossou-Niedercorn, F. *C. R. Chim.* **2013**, *16*, 311.
(35) Wang, J.; Li, P.-F.; Chan, S. H.; Chan, A. S. C.; Kwong, F. Y. *Tetrahedron Lett.* **2012**, *53*, 2887.
(36) Yamazaki, S.; Yamamoto, M.; Sumi, A. *Tetrahedron* **2007**, *63*, 2320.
(37) Palacios, F.; Vicario, J.; Aparicio, D. *Eur. J. Org. Chem.* **2006**, *2006*, 2843.
(38) Wu, Y.-J. *Tetrahedron Lett.* **2006**, *47*, 8459.
(39) Zou, B.; Jiang, H.-F. *Chin. J. Chem.* **2008**, *26*, 1309.
(40) Popov, A. F.; Perepichka, I. F.; Kostenko, L. I. *J. Chem. Soc., Perkin Trans. 2* **1989**, 395.
(41) Pardo, L.; Osman, R.; Weinstein, H.; Rabinowitz, J. R. *J. Am. Chem. Soc.* **1993**, *115*, 8263.
(42) Satterthwait, A. C.; Jencks, W. P. *J. Am. Chem. Soc.* **1974**, *96*, 7018.
(43) Wang, L.-H.; Zipse, H. *Liebigs Ann.* **1996**, *1996*, 1501.
(44) De Donder, T.; Van Rysselberghe, P. *Thermodynamic theory of affinity*; Stanford university press, 1936; Vol. *1*.
(45) Chen, W.; Yu, W.-G.; Shi, H.-B.; Lu, X.-Y. *Chemical Papers* **2012**, *66*, 308.
(46) Medina, F.; Michon, C.; Agbossou-Niedercorn, F. *Eur. J. Org. Chem.* **2012**, *2012*, 6218.
(47) Siani, G.; Angelini, G.; De Maria, P.; Fontana, A.; Pierini, M. *Org. Biomol. Chem.* **2008**, *6*, 4236.
(48) Kanzian, T.; Nigst, T. A.; Maier, A.; Pichl, S.; Mayr, H. *Eur. J. Org. Chem.* **2009**, *2009*, 6379.
(49) Desmet, G. B.; D'hooge, D. R.; Sabbe, M. K.; Marin, G. B.; Du Prez, F. E.; Espeel, P.; Reyniers, M.-F. *J. Org. Chem.* **2015**, *80*, 8520.
(50) Frisch, M. J.; Trucks, G. W.; Schlegel, H. B.; Scuseria, G. E.; Robb, M. A.; Cheeseman, J. R.; Scalmani, G.; Barone, V.; Mennucci, B.; Petersson, G. A.; Nakatsuji, H.; Caricato, M.; Li, X.; Hratchian, H. P.; Izmaylov, A. F.; Bloino, J.; Zheng, G.; Sonnenberg, J. L.; Hada, M.; Ehara, M.; Toyota, K.; Fukuda, R.; Hasegawa, J.; Ishida, M.; Nakajima, T.; Honda, Y.; Kitao, O.; Nakai, H.; Vreven, T.; Montgomery, J. A.; Peralta, J. E.; Ogliaro, F.; Bearpark, M.; Heyd, J. J.; Brothers, E.; Kudin, K. N.; Staroverov, V. N.; Kobayashi, R.; Normand, J.; Raghavachari, K.; Rendell, A.; Burant, J. C.; Iyengar, S. S.; Tomasi, J.; Cossi, M.; Rega, N.; Millam, J. M.; Klene, M.; Knox, J. E.; Cross, J. B.; Bakken, V.; Adamo, C.; Jaramillo, J.; Gomperts, R.; Stratmann, R. E.; Yazyev, O.; Austin, A. J.; Cammi, R.; Pomelli, C.; Ochterski, J. W.; Martin, R. L.; Morokuma, K.; Zakrzewski, V. G.; Voth, G. A.; Salvador, P.; Dannenberg, J. J.; Dapprich, S.; Daniels, A. D.; Farkas; Foresman, J. B.; Ortiz, J. V.; Cioslowski, J.; Fox, D. J. *Gaussian 09*; Gaussian, Inc.: Wallingford CT, 2009.
(51) Marenich, A. V.; Cramer, C. J.; Truhlar, D. G. *J. Phys. Chem. B* **2009**, *113*, 6378.
(52) Schlegel, H. B. *J. Comput. Chem.* **1982**, *3*, 214.
(53) Izgorodina, E. I.; Coote, M. L. *J. Phys. Chem. A* **2006**, *110*, 2486.
(54) Izgorodina, E. I.; Coote, M. L. *Chem. Phys.* **2006**, *324*, 96.
(55) Zhao, Y.; Truhlar, D. G. *Theor. Chem. Acc.* **2008**, *119*, 525.
(56) Krenske, E. H.; Petter, R. C.; Zhu, Z.; Houk, K. N. *J. Org. Chem.* **2011**, *76*, 5074.
(57) Ribeiro, R. F.; Marenich, A. V.; Cramer, C. J.; Truhlar, D. G. *J. Phys. Chem. B* **2011**, *115*, 14556.
(58) Scott, A. P.; Radom, L. *J. Phys. Chem.* **1996**, *100*, 16502.
(59) McQuarrie, D. A.; Simon, J. D. *Physical chemistry: a molecular approach*; Sterling Publishing Company, 1997; Vol. *1*.
(60) Klamt, A.; Eckert, F. *Fluid Phase Equilib.* **2000**, *172*, 43.
(61) Diedenhofen, M.; Eckert, F., Hellweg, A.; Huniar, U.; Klamt, A.; Loschen, C.; Reinisch, J.; Schroer, A.; Steffen, C.; Thomas, K.; Wichmann, K.; Ikeda, H. *COSMOlogic*; COSMOlogic GmbH & Co. KG: Leverkusen, 2013.
(62) D'Hooge, D. R.; Reyniers, M.-F.; Marin, G. B. *Macromol. React. Eng.* **2013**, *7*, 362.
(63) Bentein, L.; D'Hooge, D. R.; Reyniers, M.-F.; Marin, G. B. *Macromol. Theory Simul.* **2011**, *20*, 238.
(64) D'hooge, D. R.; Van Steenberge, P. H. M.; Reyniers, M.-F.; Marin, G. B. *Prog. Polym. Sci.* **2016**, *58*, 59.
(65) Smoluchowski, M. *Z. Phys. Chemie* **1917**, 129.
(66) Liu, X.; Bardow, A.; Vlugt, T. J. H. *Ind. Eng. Chem. Res.* **2011**, *50*, 4776.
(67) Pranami, G.; Lamm, M. H. *J. Chem. Theory Comput.* **2015**, *11*, 4586.
(68) Allinger, N. L.; Yuh, Y. H.; Lii, J. H. *J. Am. Chem. Soc.* **1989**, *111*, 8551.
(69) Ponder, J. W.; Richards, F. M. *J. Comput. Chem.* **1987**, *8*, 1016.
(70) Petzold, L. *Siam J. Sci. Stat Comput* **1983**, *4*, 136.

DOI: 10.1021/acs.joc.6b02218
J. Org. Chem. 2016, 81, 12291−12302